Chapter 2

Structure and Physical Properties of $59B_2O_3$–$10Na_2O$–(30 – x)CdO–xZnO–1CuO (0 ≤ x ≤ 30) Glass System

L.S. Ravangave and G. N. Devde

Additional information is available at the end of the chapter

http://dx.doi.org/10.5772/intechopen.73865

Abstract

A series of stable and transparent glasses with the composition $59B_2O_3$–$10Na_2O$–(30 − x) CdO–xZnO–1CuO (0 ≤ x ≤ 30) (where x = 0, 7.5, 15, 22.5, and 30 mol%) were prepared by conventional melt-quenching technique. These glasses were characterized using X-ray diffraction (XRD), Fourier-transform infrared (FTIR) and Raman spectroscopes, differential scanning calorimetry (DSC), optical absorption, and electron paramagnetic resonance (EPR). XRD and DSC analysis confirmed the glassy nature of the prepared samples. The physical properties such as density (ρ), molar volume (V_m), oxygen packing density (OPD), and the molar volume of oxygen (V_o) were calculated and discussed. FTIR and Raman studies showed that the glass network consists of BO_3 and BO_4 units in various borate groups. From DSC, it was found that the glass transition temperature (T_g) varies nonlinearly with the addition of ZnO content in place of CdO. Both EPR and optical absorption results have confirmed that the Cu^{2+} ions are in octahedral coordination with a strong tetrahedral distortion. The changes in various spectroscopic properties of Cu^{2+} ions in the glasses such as spin-Hamiltonian parameters ($g_\parallel$, $g_\perp$ and $A_\parallel$) and bonding coefficients (α^2, β_1^2, and β^2) were understood with the help of FTIR and Raman studies.

Keywords: glasses, DSC, Raman, FTIR, EPR

1. Introduction

Alkali borate systems are attractive materials from a fundamental point of view as well as technological point of view [1]. From the literature, it has been observed that certain borate glasses are of greater interest and relevance because of their suitability in the progress of waveguides, electro-optic switches and modulators, magneto-optic materials, and solid-state

laser materials [2]. B_2O_3–ZnO glass has a high transparent window in the region from 370 nm to 2.2 μm, and these glasses are attractive host materials to incorporate rare earth elements for optoelectronics and optical fibers [3, 4]. The properties of B_2O_3 glass can often be altered by the addition of network modifiers. The most commonly used network modifiers are the alkali (Li_2O, Na_2O, and K_2O) and alkaline earth oxides (MgO, CaO, SrO, and BaO) [5, 6]. When mixed with these glass modifiers, its internal structure is rearranged due to the formation of non-bridging oxygen [7]. In particular, the addition of alkali oxide to pure B_2O_3 causes a progressive change of the boron atom coordination number (CN), from 3 (BO_3) to 4 (BO_4), and results in the formation of various borate units (diborate, triborate, tetraborate groups, etc.) [1].

From the literature, it was found that with the presence of ZnO or CdO in B_2O_3 glass matrix, UV transmission ability could be enhanced [8]. Therefore the authors have selected Na_2O, CdO, and ZnO as network modifiers. The addition of Cd and Zn oxides also results in the large glass formation domain [9]. When zinc oxide is introduced to borate glasses, there are two ways in which zinc ion can get incorporated into the glass. Zinc oxide may act as a network modifier by disrupting the bonds connecting neighboring [BO_3] and [BO_4] groups. On the other hand, zinc oxide can be incorporated into the glass as [ZnO_4] structural units. Besides Cu^{2+} ions have been chosen in the present study as an EPR probe due to its EPR spectrum being sensitive enough to detect minute changes in the structure of the glasses [10]. Therefore in this article, authors have been presented the structural changes of Cu^{2+} ions-doped B_2O_3–Na_2O–CdO–ZnO glass induced by addition of ZnO into B_2O_3 glass matrix at 10 mol% Na_2O content. The various literature surveys show no evidences on structural study using FTIR, Raman spectroscopy, EPR, and optical absorption. Therefore the authors have planned to investigate the structural, optical, and physical changes in the Cu^{2+} ions-doped B_2O_3–Na_2O–CdO–ZnO glass system. The authors have also studied the spin-Hamiltonian parameters and site symmetry around Cu^{2+} ions in these glasses using EPR and optical absorption studies. The variations in the thermal properties and other physical properties in terms of structural changes of glasses have been discussed [6].

2. Experimental

2.1. Glass preparation

Glasses with compositional formula $59B_2O_3$–$10Na_2O$–(30 − x)CdO–xZnO–1CuO (where x = 0, 7.5, 15, 22.5, and 30 mol%) were prepared using melt-quenching technique, and a series of glasses along with their codes are given in **Table 1**. All the chemicals used were of 99% purity from well-known companies (sd-fine, Merck, and Loba Chemie).

Appropriate amounts of H_3BO_3, Na_2CO_3, ZnO, and CdO were ground with a mortar and pestle and thoroughly mixed. About 1 mol% CuO was added as a spin probe and was melted in a platinum crucible at 1000°C for 30 min in an Autoset electric furnace; a similar technique was employed by Devde et al. [6].

http://dx.doi.org/10.5772/intechopen.73865

Sample code	Composition (mol%)
BNCZ1	$59B_2O_3$–$10Na_2O$–30CdO
BNCZ2	$59B_2O_3$–$10Na_2O$–22.5CdO–7.5ZnO
BNCZ3	$59B_2O_3$–$10Na_2O$–15CdO–15ZnO
BNCZ4	$59B_2O_3$–$10Na_2O$–7.5CdO–22.5ZnO
BNCZ5	$59B_2O_3$–$10Na_2O$–30ZnO

Table 1. Glass compositions of $59B_2O_3$–$10Na_2O$–(30 − x)CdO–xZnO–1CuO (0 ≤ x ≤ 30 mol%) glass system.

During the melting the crucible with homogeneous mixture was covered with a lid to avoid the volatility of the powder compounds or contamination from the furnace. Melts were stirred frequently to promote homogeneity, and the liquids were rapidly poured into a mold made with a stainless steel which was maintained at 200°C and pressed with another stainless steel plate maintained at the same temperature. The prepared glass samples were then transferred to another furnace and annealed at 300°C for 6 h to relieve thermal stress and strains of the glass samples. The prepared samples were examined, and it was found that the samples are clear, bubble free, and transparent.

2.2. Physical properties

Archimedes' method using xylene as immersion liquid was employed for the measurement of densities of the prepared glasses at room temperature. An average of three samples of each glass code was used. Obtained density values were used to calculate the molar volume using relation $V_m = M/\rho$, where M and ρ are the average molecular weight and density of the glasses, respectively. Oxygen packing density (OPD) was calculated using the relation $OPD = \Sigma x_i n_i / V_m$, where x_i is the molar fraction of an oxide R_mO_n and n_i is the number of oxygen atoms of this oxide [6]. The molar volume of oxygen (V_o) is the volume of glass in which 1 mole of oxygen is contained. These values were calculated using the relation $V_o = (V_m)(1/\Sigma x_i n_i)$.

Various spectroscopic techniques were employed for structure investigation of present glass system.

2.3. XRD

X-ray diffraction patterns of the glass samples were recorded from Philips diffractometer (PANalytical X-pert PRO model) with Cu K_α (1.54 Å) source at room temperature.

2.4. FTIR studies

The infrared transmission spectra of all glasses were recorded at room temperature in the wave number range 400–1800 cm^{-1} by a Shimadzu FTIR-8001 Fourier-transform computerized infrared spectrometer. The IR transmission measurements were made using the KBr pellet technique.

2.5. Raman studies

Raman spectra of all prepared glasses were recorded at room temperature in the range 200–1800 cm^{-1} using a He–Ne excitation source (632.81 nm) coupled with Jobin Yvon Horiba (LABRAM HR-800) micro Raman spectrometer equipped with a 50× objective lens to focus the laser beam. The incident laser power was focused in a diameter of ~1–2 μm, and a notch filter was used to suppress Rayleigh light. Samples used for the measurement were of 1 mm thickness and 1 cm in diameter. Raman shifts are measured with a precision of ~0.3 cm^{-1}, and the spectral resolution is of the order 1 $cm^{-}1$; a similar characterization was studied by Upender et al. [11].

2.6. DSC studies

Differential scanning calorimetry of the prepared glass powders was carried out at temperatures up to 850°C at the rate of 10°C/min using a SETARAM instrument (Model LABSYS EVO DSC; SETARAM Instrumentation, Caluire, France) to determine the thermal properties of the glasses [6].

2.7. EPR studies

JEOL-JES FE 3X EPR spectrometer was employed for recording EPR spectra of the glass samples in the X-band at room temperature with 100 kHz field modulation. Polycrystalline diphenyl picryl hydrazyl (DPPH) was used as the standard "g" marker for the determination of magnetic field; a similar technique was employed by G. Upender et al. for invention of structure of WO_3–GeO_2–TeO_2 glasses [12].

2.8. UV-Visible absorption studies

UV-Visible absorption spectra of prepared borate-based glasses were recorded by using LABINDIA Analytical UV-3092 spectrophotometer in the wavelength range 350–900 nm at room temperature. The precision of wavelength measurement is about ±1 nm [12].

3. Results and discussion

3.1. Basic glass properties

The physical parameters of the present glasses are presented in **Table 2**. It is observed that the density (ρ) decreases from 3.334 to 2.815 g/cm^3 with the addition of ZnO content from 0 to 30 mol% at the expense of CdO content. This could be due to the lower molecular weight of ZnO (81.38 g/mol) in comparison with CdO (128.4 g/mol). This could also be due to the lower density of ZnO (ρρ = 5.606 g/cm^3) than that of CdO (ρ ρ= 6.95 g/cm^3).

The molar volume (V_m) increases from 25.972 to 26.224 cm^3/mol with ZnO content up to 15 mol% then V_m starts decreasing from 26.224 to 25.995 and then to 25.749 with further

Parameter	x = 0	x = 7.5	x = 15	x = 22.5	x = 30
*AMW (g/mol)	86.589	83.062	79.536	76.009	72.483
ρ (g/cc) (±0.005)	3.334	3.181	3.033	2.924	2.815
†V_m (cm^3/mol)	25.972	26.112	26.224	25.995	25.749
OPD (mol/l)	83.936	83.487	83.129	83.862	84.663
V_o (cm^3/mol)	11.914	11.978	12.029	11.924	11.812

*AMW: average molecular weight.
†Error in V_m is ±0.005.

Table 2. Physical parameters of $59B_2O_3$–$10Na_2O$–(30 − x)CdO–xZnO–1CuO (0 ≤ x ≤ 30 mol%) glass system.

addition of ZnO up to 30 mol% at the expense of CdO. This could be due to the difference between cation radii of Cd^{2+} ion (1.03 Å) and Zn^{2+} ion (0.83 Å). The nonlinear variation in V_m also suggests the dual role of ZnO content as in the present system ZnO up to 15 mol%, it plays a modifier role, and beyond it plays a glass former role. It is also observed that the oxygen packing density (OPD) decreases from 83.936 to 83.129 mol/l, while oxygen molar volume (V_o) increases from 11.914 to 12.029 cm^3/mol with ZnO content up to 15 mol%. But OPD increases from 83.129 to 84.663, while V_o decreases from 12.029 to 11.812 with ZnO addition up to 30 mol%. The nonlinear variation in OPD and V_o values with the increase in ZnO content from 0 to 30 mol% could be due to the variation in density (ρ) and the dual role of ZnO in the present glass system, while the number of oxygen atoms in the glass network remains the same according to the ratio 1:1.

3.2. XRD

The obtained XRD patterns of BNCZ glass system are shown in **Figure 1**. It is clear that a broad hump is repeatedly observed in all the samples and is the characteristic of glass, and there is no evidence of crystallization. Hence it is confirmed that the prepared samples possess glassy nature.

3.3. FTIR studies

The IR transmission spectra of all the glasses were recorded in the wave number range 1600–400 cm^{-1} and are shown in **Figure 2**. The band positions and their assignments are given in **Table 3**.

In the BNCZ glass system, significant bands are observed at about ~474, 694, 970–1040, 1250–1260, and 1360–1375 cm^{-1}. These bands assigned to B_2O_3 and about 80% of the boron atoms are present in the boroxol rings, B_3O_6, that are interconnected by independent BO_3 groups. The vibrational modes of the vitreous borate network are mainly active in three infrared regions. The IR features located in the first region that ranges between 1200 and 1600 cm^{-1} [13]. The second region ranges between 800 and 1200 cm^{-1}, and the third region ranges between 600 and 800 cm^{-1}. From **Figure 2** it is evidently seen that the structure of the glass network formed

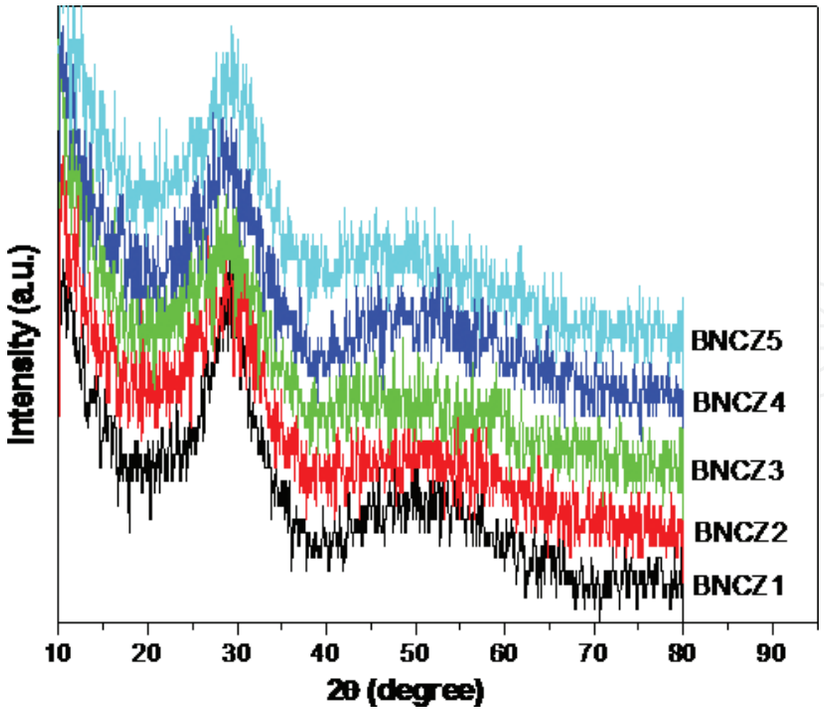

Figure 1. XRD patterns of $59B_2O_3$–$10Na_2O$–(30 − x)CdO–xZnO–1CuO (0 = x = 30 mol%) glass system.

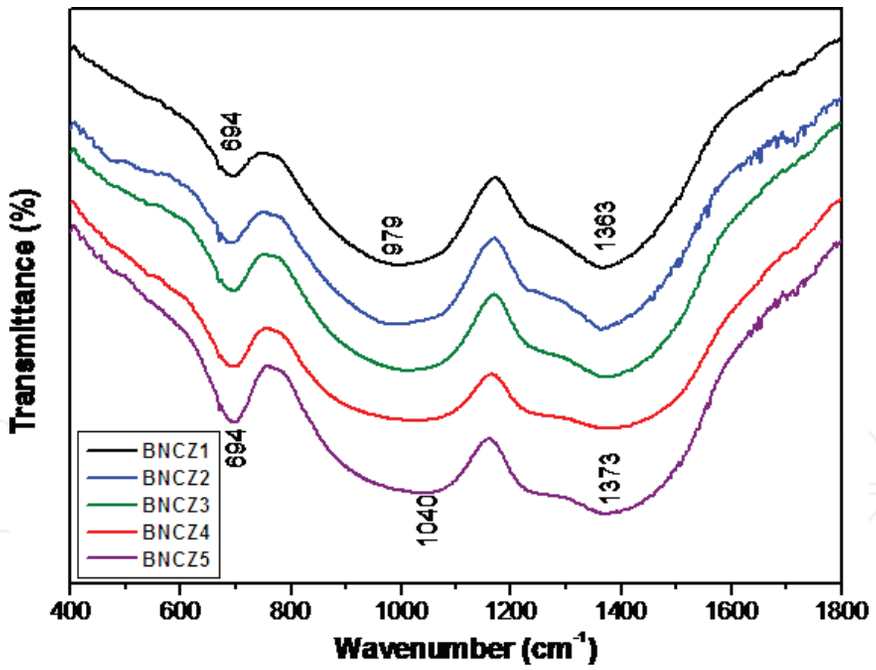

Figure 2. IR spectra of $59B_2O_3$–$10Na_2O$–(30 − x)CdO–xZnO–1CuO (0 = x = 30 mol%) glass system.

by boron ions is significantly changed with the incorporation of ZnO at the expense of CdO content. The absence of IR band at ~806 cm^{-1} indicates that the boroxol rings are not formed in the present glass system, and hence the structure of the glasses consists of borate groups other than the boroxol rings. The weak band observed at ~474 cm^{-1} in all the glasses is attributed to the vibration of metal cations in their oxygen sites (RO_4 groups where R = Cd, Zn) [16].

Band positions	Assignment
1360–1375	Symmetric stretching vibrations of B–O bonds of trigonal $(BO_3)^{3-}$ units in Meta, Pyro and ortho borates
1260	Symmetric stretching vibrations of B–O of $(BO_3)^{3-}$ units in meta and Ortho Borates
1040	B–O stretching vibrations of BO_4 units in tri, tetra and penta borate groups
970	B–O asymmetric stretching of BO_4 units of diborate groups
690	Bending vibrations of B–O–B linkages in borate network

Table 3. Band positions and assignments of IR bands of $59B_2O_3$–$10Na_2O$–(30 − x)CdO–xZnO–1CuO (0 ≤ x ≤ 30 mol%) glass system.

The bands observed around 694 cm^{-1} could be attributed to the bending vibration of B–O–B linkages of various borate groups [17]. The bands near 979 cm^{-1} are assigned to B–O asymmetric stretching of BO_4 units of diborate groups [18]. This band shifts to higher wave number side, i.e., from 979 to 1040, while the intensity of this band significantly decreased with the increase of ZnO content up to 30 mol%. The bands observed at around 1040 cm^{-1} are due to B–O stretching vibrations of BO_4 units in tri-, tetra-, and pentaborate groups [12, 19, 20]. The bonds that appeared in the range of 1260 cm^{-1} are assigned to B–O symmetric stretching vibrations of $(BO_3)^{3-}$ units in metaborate and orthoborates [21]. The intensity of this band is unaffected with the addition of ZnO content up to 30 mol%. The bands at around 1363–1375 cm^{-1} could be attributed due to symmetric stretching vibrations of B–O bonds of trigonal $(BO_3)^{3-}$ units in meta-, pyro-, and orthoborates [21, 22]. The broadness of these bands was found to be more with the substitution of ZnO content up to 30 mol%. The B_2O_3 is built up of BO_3 triangles, and upon adding ZnO, the coordination number of the boron changes from SP^3 tetrahedral BO_4 to form SP^2 planar BO_3, preserving the B–O bonding without the creation of non-bridging oxygen ions. It means that the introduction of ZnO causes a significant formation of the BO_3 groups with a lower coordination number. Therefore, the progressive increase in ZnO content makes the IR bands observed at about 1040 and1373 cm^{-1} more pronounced. This means that the BO_3 groups and hence the bridging oxygen contents are increased with increasing of ZnO content on the expenses of CdO content.

3.4. Raman studies

Figure 3 shows the Raman spectra of the present glass system in the spectral range 200–1800 cm^{-1} consisting of sharp, broad peaks and shoulders.

The Raman peak positions are summarized in **Table 4**.

The Raman spectrum of vitreous B_2O_3 is dominated by a strong peak centered at ~804 cm^{-1}. The ~804 cm^{-1} peak is assigned to the boroxol ring breathing vibration involving little motion of boron [23–25]. The desired peak at ~ 804 cm^{-1} was not appeared and therefore boroxol rings are absent in the present glass system. Therefore, boroxol ring is absent in these glasses. The Raman peak at around 447–470 cm^{-1} is assigned to pentaborate and diborate groups [26]. The weak Raman peak appearing at ~697 cm^{-1} is due to metaborate/$(BO_3)^{3-}$ vibrations [27, 28]. The strong peak at around ~770 cm^{-1} is assigned to symmetric breathing vibrations of six-membered

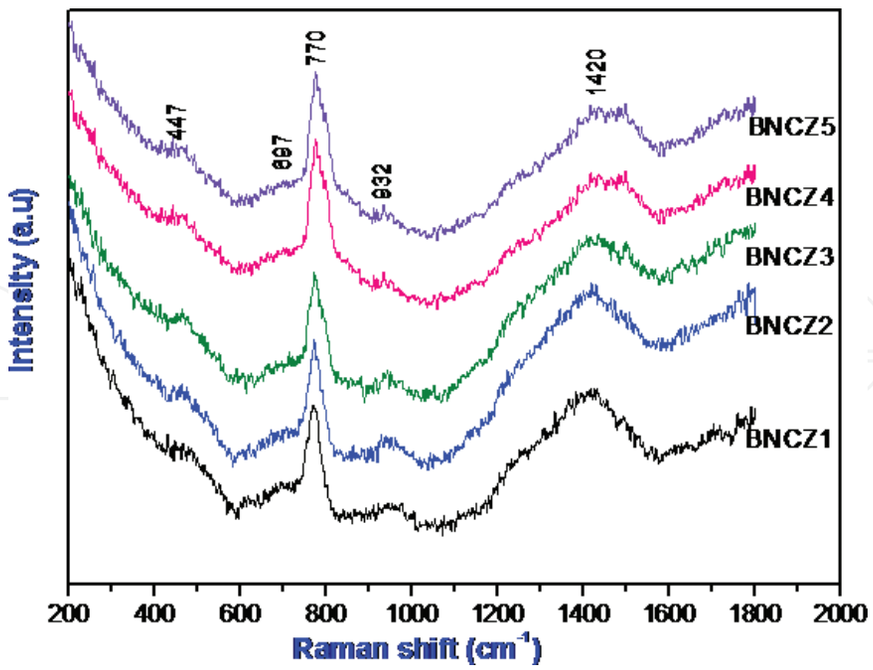

Figure 3. Raman spectra of $59B_2O_3$–$10Na_2O$–(30 − x)CdO–xZnO–1CuO (0 = x = 30 mol%) glass system.

Sample code	Raman peaks (cm^{-1})				
BNCZ1	470	697	770	948	1420
BNCZ2	464	697	770	943	1420
BNCZ3	464	697	770	942	1420
BNCZ4	457	697	770	935	1420
BNCZ5	447	697	770	932	1420

Table 4. Raman peak positions of $59B_2O_3$–$10Na_2O$–(30 − x)CdO–xZnO–1CuO (0 ≤ x ≤ 30 mol%) glass system, with error ±1 cm^{-1}.

rings with both BO_3 triangles and BO_4 tetrahedra (tri-, tetra-, or pentaborate groups) [29, 30]. The intensity of this peak is significantly increased with the addition of ZnO content up to 30 mol%. This observation suggests more number of BO_3 units instead of BO_4 units in six-membered rings. No Raman peaks appeared at around ~ 834 cm^{-1} in any of the glass, and it indicates that there are no pyroborate groups ($B_2O_5^{4-}$) present in these glasses. The pentaborate and tetraborate groups were assigned by the peaks observed in the range ~930–950 of Raman spectrum. The broad band around 1420 cm^{-1} was assigned to the B–O^- bonds attached to the large number of borate groups [31, 32]. The decrease in intensity of the peak at ~1420 cm^{-1} is due to increase of ZnO content up to 30 mol%. This shows that significant formation of Zn^{2+}-B–O^- bonds by reducing the number of non-bridging oxygen's (NBO's) similar finding was recorded by Upentre et al. for the glass system (90–x)TeO2–10GeO2–xWO 3 (7.5 ≤ x ≤ 30) doped with Cu^{2+} ions [33]. The observed slight decrease in intensity and shift in the peak ~470 toward lower wave number (447 cm^{-1}) indicates the decrease of penta- or diborate groups in the glasses. The intensity of the peak at ~940 cm^{-1} decreases while shifts to lower wave number

from 948 to 943, 942, 935, and then 932 with increase in ZnO content. This may indicate the presence of less number of pentaborate groups and bond lengths of B–O bonds of pentaborate groups could be increased. The above results suggest the presence of more BO_3 units in the glasses with the addition ZnO as Zn^{2+} establishes the linkages of NBOs with BO_4 units.

3.5. Differential scanning calorimetry (DSC)

The DSC thermograms of the present glasses are shown in **Figure 4**. Glass transition temperature (T_g) is always visible, and this result is in agreement with the result of XRD data as both the techniques confirm the glassy nature of the samples.

The values of glass transition temperature (T_g) are given in **Table 5**.

From this table it is observed that T_g decreases from 497 to 488°C with gradual increase in ZnO content up to 15 mol% at the expense of CdO, and thereafter T_g increases from 488 to 492 and then to 496°C with further addition of ZnO up to 30 mol%. This behavior suggests that T_g varies nonlinearly with the addition of ZnO content in place of CdO. It is well known that a higher cation radius of Cd^{2+} (1.03 Å) replaced with a lower cation radius of Zn^{2+} (0.83 Å) decreases the overall cation polarizability (polarizability is proportional to the cation size); as a result, T_g should decrease linearly with ZnO content. On the contrary to this, the bond strength of Zn–O (151 kJ/mol) is more than that of Cd–O (101 kJ/mol) [33]; as a result, T_g should increase linearly. But none of the reasons are suitable in this case. Therefore, the observed nonlinear variation in T_g with ZnO content can be understood in the following way: As it was observed clearly from FTIR and Raman that more numbers of BO_4 units are present up to 15 mol% of ZnO, then with further addition of ZnO in place of CdO up to 30 mol%,

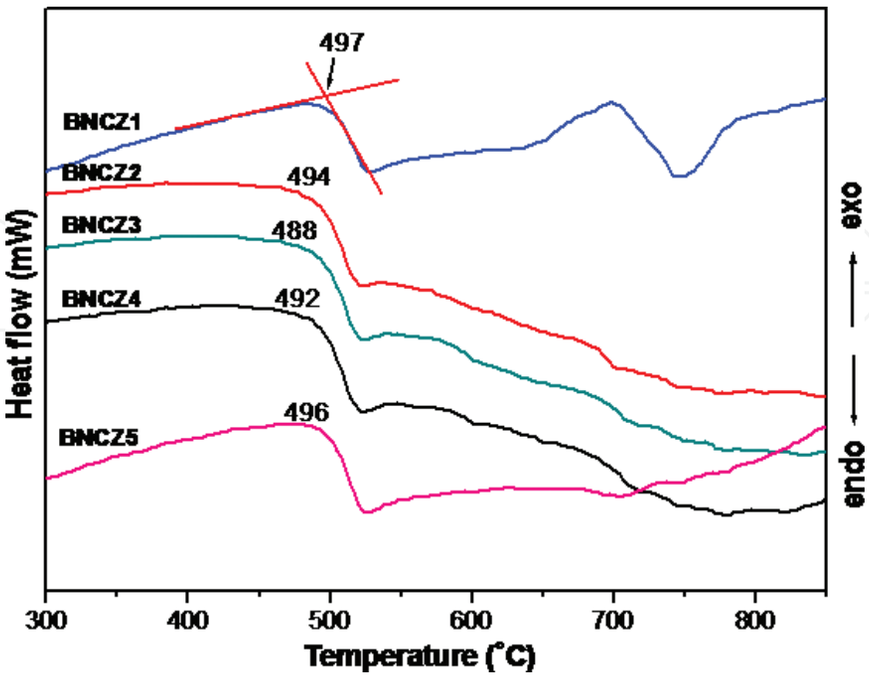

Figure 4. DSC curves of $59B_2O_3$–$10Na_2O$–(30 − x)CdO–xZnO–1CuO (0 = x = 30 mol%) glass system. Heating rate was 10°C/min.

Sample code	Glass Transigirían temperature T_g (°C)
BNCZ1	497
BNCZ2	494
BNCZ3	488
BNCZ4	492
BNCZ5	496

Table 5. Glass Transigirían temperature T_g (°C) for compositions of $59B_2O_3$–$10Na_2O$–(30 − x)CdO–xZnO–1CuO (0 ≤ x ≤ 30 mol%) glass system.

most of BO_4 units are converted to BO_3 units. The bond strength of BO_4 units (373 kJ/mol) is smaller than BO_3 units (498 (kJ/mol%) [34]. Hence, T_g decreases up to 15 mol% of ZnO and then starts increasing with further addition of ZnO up to 30 mol%. Besides this the higher field strength of Zn^{2+} ions (0.53 cm^{-2}) than that of Cd^{2+} ions (0.38 cm^{-2}) in the glass network also causes to increase the T_g [34]. However, the ionicities of both Zn–O (51%) and Cd–O (51%) are the same, and its role could be neglected. From **Figure 4** it is clearly seen that except in BNCZ1 the onset crystallization temperature (T_o) is not prominently observed with the incorporation of ZnO content. This indicates that the increase of ZnO in place of CdO has a tendency to prevent crystallization. Thus, the present glasses are more thermally stable against crystallization.

3.6. EPR studies

The electron paramagnetic resonance spectra of Cu^{2+}-doped BNCZ series are shown in **Figure 5**. It is essential to dope the glass samples with Cu^{2+} ions as this gives resonance signals; a similar work is reported in earlier literature [35–37]. The copper ions with spin 1/2 gives a nuclear spin I = 3/2 for ^{63}Cu and ^{65}Cu and therefore results in (2I + 1) hyperfine components, i.e., four parallel and four perpendicular components.

The spectra recorded for prepared glass series exhibit three parallel components in the lower field region and one parallel component which is overlapped with the perpendicular component. The EPR spectra of copper ions in all the glass samples have been analyzed using an axial spin-Hamiltonian in which the quadrupole and nuclear Zeeman interaction terms are ignored.

$$H = g_{\parallel}\beta H_z S_z + g_{\perp}\beta (H_x S_x + H_y S_y) + A_{\parallel} S_z I_z + A_{\perp} (S_x I_x + S_y I_y) \quad (1)$$

The symbols have their usual meaning.

The solution to the spin-Hamiltonian gives the expressions for the peak positions related to the principal values of g and A tensor as follows [35–37].

For parallel hyperfine peaks,

$$h\nu = g_{\parallel}\beta H_{\parallel} + mA_{\parallel} + (15/4 - m^2)\, A_{\perp}^2 / 2g_{\parallel}\beta H_{\parallel} \quad (2)$$

http://dx.doi.org/10.5772/intechopen.73865

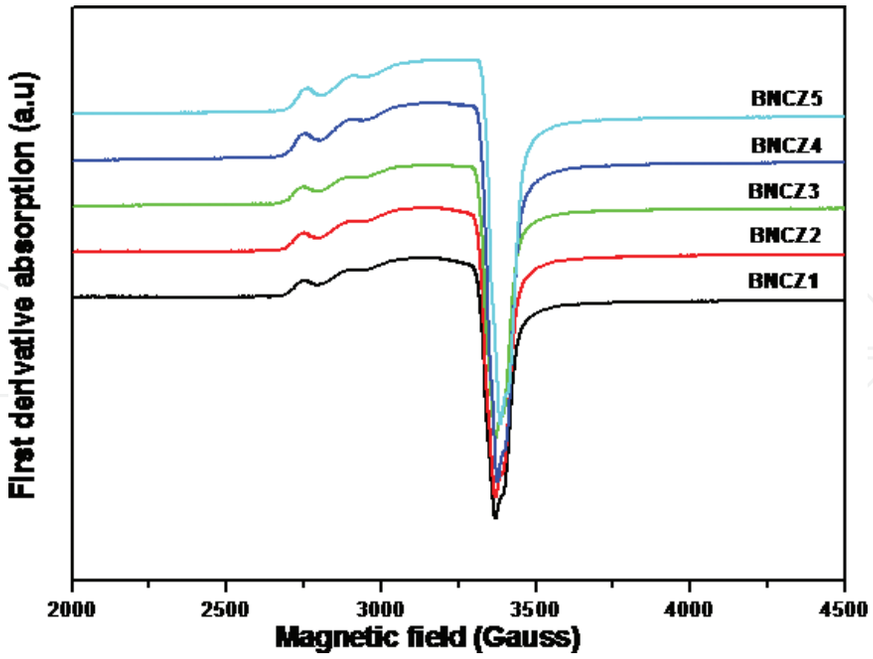

Figure 5. EPR spectra of $59B_2O_3$–$10Na_2O$–(30 − x)CdO–xZnO–1CuO (0 = x = 30 mol%) glass system at room temperature.

For perpendicular hyperfine peaks,

$$h\nu = g_{\perp}\beta H_{\perp} + mA_{\perp} + (15/4 - m^2)\,(A_{\perp}^2 + A_{\parallel}^2)/4g_{\perp}\beta H_{\perp} \quad (3)$$

The symbols have the usual meaning. Using Eqs. (2) and (3), the spin-Hamiltonian parameters of all the glasses have been calculated and are tabulated as shown in **Table 6** [12].

From **Table 6**, the $g_{\parallel}$, $g_{\perp}$ and $A_{\parallel}$ values are found to be dependent on the glass composition. It is found that $g_{\parallel} > g_{\perp} > g_e$ (where $g_e = 2.0023$ is free electron g-value). Therefore from the $g_{\parallel}$ values and shape of the EPR spectra, it can be concluded that the ground state of the Cu^{2+} is d_{x2-y2} orbital $^2B_{1g}$ state, the Cu^{2+} ions are located in tetragonally distorted octahedral sites [35–37]. The changes in the spin-Hamiltonian parameters with varying ZnO content in the place of CdO content are attributed to the change in electron cloud density around the Cu^{2+} ions in the glass network. The change in electron cloud density can be understood in the following way: From FTIR and Raman structural analysis, it was observed that the structure of the glasses changed with the incorporation of ZnO content from 0 to 30 mol%. The increasing ZnO content from 0 to 30 mol% to B_2O_3 glass network leads to change the coordination number of certain boron atoms from 4 to 3. Thus it is understood that every glass composition of the glass system is composed of both triangular (BO_3) and tetrahedral (BO_4) units. Therefore, some of the Cu^{2+} ions are surrounded by these groups containing NBOs which may present varied electron cloud density around Cu^{2+} site in the form of CuO_6 and hence the variations in the spin-Hamiltonian parameters as observed in the present glass system. The variations in EPR parameters not only depend on the above said reasons but also depend on the differences in the field strengths of various cations (B^{3+} (1.39 cm^{-2}), Na^+ (0.18 cm^{-2}), Cd^{2+} (0.38 cm^{-2}), and Zn^{2+} (0.53 cm^{-2})) as well as the cation polarizabilities of Na^+ ions

Glass code	$g_{\parallel}$	$g_{\perp}$	$A_{\parallel}(\times 10^{-4}\ cm^{-1})$
BNCZ1	2.323	2.064	147
BNCZ2	2.322	2.068	147
BNCZ3	2.325	2.066	148
BNCZ4	2.327	2.069	146
BNCZ5	2.326	2.068	147

Table 6. Spin-Hamiltonian parameters (SHP) of $59B_2O_3$–$10Na_2O$–$(30 - x)CdO$–$xZnO$–$1CuO$ ($0 \le x \le 30$ mol%) glass system.

(0.181 Å^3), Zn^{2+} ions (0.283 Å^3), Cd^{2+} ions (1.087 Å^3), and B^{3+} ions (0.002 Å^3) [6] that cause the fluctuations in the ligand field around Cu^{2+} ions, and this in turn varies the spin-Hamiltonian parameters as observed.

3.7. Optical absorption studies

The UV-Visible absorption spectra of prepared glass series were displaced in **Figure 6**.

The observed absorption band around ~765 nm in BNCZ1 is assigned to the $^2B_{1g} \rightarrow {}^2B_{2g}$ transition (ΔE_{xy}) of Cu^{2+} ion in octahedral coordination with a strong tetrahedral distortion, and the EPR results were found to be in agreement with this assumption [36]. From **Figure 6**, it was found that the absorption peak firstly blueshifted, i.e., from 764 to 760 and then to 756 nm with the addition of ZnO up to 15 mol%, and then redshifted, i.e., from 756 to 760 to 763 nm with the further addition of ZnO from 15 to 30 mol%. This result is consistent with the observations made in FTIR, Raman, and DSC. As pointed out by Raman and IR analysis, the major structural changes in the present glass take place with the addition of divalent ZnO. This consequence suggests that ZnO enters the glass system in the form of network modifier. Hence, all the observations are clearly from tetragonal (BO_4) to trigonal (BO_3) units with the incorporation of ZnO content at the expense of CdO content.

The variation in peak position with ZnO doping in glass system BNCZ (30 mol%) indicates the change in the ligand field around paramagnetic Cu^{2+} ions. This could be due to higher field strength of Zn^{2+} ions (0.53 cm^{-2}) than that of Cd^{2+} ions (0.38 cm^{-2}) [33]. The change in polarizability of oxygen ions surrounding the Cu^{2+} may also change the peak position [6]. This can be understood as follows. As ZnO content substitutes CdO content from 0 to 30 mol%, from IR and Raman structural analysis, it was observed that ZnO has played the dual role. Thus, during the modifier role of ZnO (up to 15 mol%), weak bonds Zn^{2+}–O–B were formed in the place of B–O–B or Cd–O–B, whereas during the former role of ZnO (from 15 to 30 mol%), strong Zn–O–B bonds were formed. Thus the oxygen ions in Zn^{2+}–$^{-}$O–B bonds are less tightly bound than in B–O–B or Cd–O–B bonds. Thus the oxygen ions can be treated as NBOs in which electrons are loosely bound to the nucleus, and hence these NBOs are more polarized than the oxygen ions in B–O–B or Cd–O–B. These NBOs are decreased during the conversion of BO_4 units into BO_3 units when ZnO started playing the former role above 15 mol%. Similar observations

http://dx.doi.org/10.5772/intechopen.73865

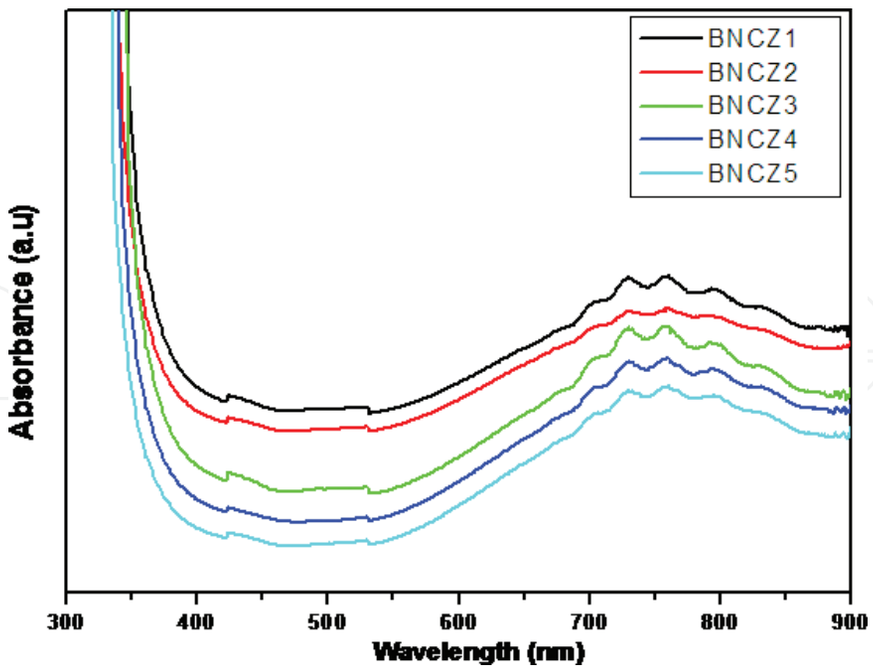

Figure 6. Optical absorption spectra of $59B_2O_3$–$10Na_2O$–(30 – x)CdO–xZnO–1CuO.

were reported by other authors [37]. With the conversion of four coordination boron atoms [BO_4] into three coordination boron atoms [BO_3], the excess of oxygen converts some of Zn^{2+} ions into tetrahedra [ZnO_4] where the structural modification in the glass network could be reason for the variation of the ligand field strength of Cu^{2+} ions. This may be the reason why the optical absorption maximum has showed the nonlinear variation with ZnO content.

3.7.1. Cu^{2+}-ligand bonding nature

The data of EPR and optical absorption can be correlated to understand the environment around Cu^{2+} ions in the present glass network; in connection to this, the bonding parameters were evaluated using EPR and optical data by the following equations [6].

$$g_{\parallel} = 2.0023(1\text{-}4\lambda\alpha^2\beta_1^2/\Delta E_{xy}) \quad (4)$$

$$g_{\perp} = 2.0023(1\text{-}\lambda\alpha^2\beta^2/\Delta E_{xz,yz}) \quad (5)$$

where ΔE_{xy} and $\Delta E_{xz,yz}$ are the energies corresponding to the transitions of $^2B_{1g} \rightarrow {}^2B_{2g}$ and $^2B_{1g} \rightarrow {}^2E_g$, respectively, and λ is the spin-orbit coupling constant (= −828 cm^{-1}) and the bonding coefficients α^2, β_1^2, and β^2 (≈1.00) characterize in-plane σ bonding 16 between the d orbital of Cu^{2+} and the p orbital of ligand, in-plane π bonding between the d orbital of Cu^{2+} and p orbital of ligand and out-of-plane π bonding between the d orbital of Cu^{2+} and p orbital of ligand in the glasses respectively [6]. Besides the values of ΔE_{xy} and $\Delta E_{xz,yz}$ are also calculated and presented in **Table 7**. In the present glasses, the bonding parameters α^2, β_1^2, and β^2 were evaluated using the following equations [38, 39] and are displayed in **Table 7**.

Parameter	x = 0	x = 7.5	x = 15	x = 22.5	x = 30
λ (nm) (±1)	764	760	756	760	763
ΔE_{xy} (cm^{-1})	13,089	13,158	13,228	13,158	13,106
$\Delta E_{xz,yz}$ (cm^{-1})	20,666	19,408	20,017	19,117	19,408
α^2	0.798	0.799	0.804	0.802	0.803
β^2	0.964	0.963	0.957	0.959	0.958
β_1^2	0.793	0.794	0.801	0.803	0.797
Γ_π (%)	41.4	41.2	39.8	39.4	40.6
Γ_σ (%)	37.33	37.15	36.22	36.59	36.41

Table 7. Bonding parameters of $59B_2O_3$–$10Na_2O$–(30 − x)CdO–xZnO–1CuO (0 ≤ x ≤ 30 mol%) glass system.

$$\alpha^2 = \left| A_{\parallel}/P \right| + (g_{\parallel}-2) + 3/7(g_{\perp}-2) + 0.04 \tag{6}$$

$$\beta_1^2 = [(g_{\parallel}/g_e) - 1]\Delta E_{xy}/4\lambda\alpha^2 \tag{7}$$

$$\beta^2 = [(g_{\perp}/g_e) - 1]\Delta E_{xz,yz}/\lambda\alpha^2 \tag{8}$$

Here P is dipolar hyperfine coupling parameter (=0.036 cm^{-1}). From Eqs. (4) and (5), in order to determine Cu^{2+} bonding coefficients, besides the EPR parameters, the energy positions of the absorption bands of Cu^{2+} which indicate the values of ΔE_{xy} and $\Delta E_{xz,yz}$ are required. Since one absorption band corresponding to $^2B_{1g} \rightarrow {}^2B_{2g}$ transition (ΔE_{xy}, are presented in **Table 7**) was observed, the position of the second band can be estimated by using the following equation [39] and the values are presented in **Table 7**.

$$\Delta E_{xz,yz}(^2B_{1g} \rightarrow {}^2E_g) = 2K^2\lambda/2.0023 - g_{\perp} \tag{9}$$

where K^2 is the orbital reduction factor ($K^2 = 0.77$) and λ is the spin-orbit coupling constant.

The normalized covalency of the Cu^{2+}–O in-plane bonding of σ and π symmetry is expressed in terms of bonding coefficients α^2 and β_1^2 as follows:

$$\Gamma_\sigma = 200(1\text{-}S)\ (1\text{-}\alpha^2)/(1\text{-}2S)\% \tag{10}$$

$$\Gamma_\pi = 200(1\text{-}\beta_1^2)\% \tag{11}$$

where S is the overlapping integral ($S_{oxy} = 0.076$). The values of Γ_σ and Γ_π are given in **Table 6**. It is clear from **Table 7** that both of these values are varied with addition of ZnO content to B_2O_3 network. This could be due to variation of structural changes within the glasses. In

http://dx.doi.org/10.5772/intechopen.73865

general if α^2 have smaller values, then the greater the covalent nature of the bonding. The calculated values of α^2 for prepared glass series (the range 0.798–0.803) suggest that the in-plane σ bonding in the glasses is moderately covalent in nature, whereas the values of β_1^2 (0.793–0.803) obtained for various glasses indicate that the in-plane π bonding is significantly ionic in nature.

The changes in this parameter can be attributed to the changes in O–X bonds (where X = B, Cd, and Zn) because it reflects the competition in the Cu^{2+}–O–X bonds, between the cupric ion and its neighboring X cations for attracting the lone pairs of the intervening oxygen ions. In the present system, the values of β^2 were found to be close to unity, and it suggests that out-of-plane π bonding is more ionic in nature and the magnitudes of all bonding parameters are comparable to those found for Cu^{2+} in other glasses [6].

4. Conclusions

Transparent glasses with composition $59B_2O_3$–$10Na_2O$–(30 − x)CdO–xZnO–1CuO (where x = 0, 7.5, 15, 22.5, and 30 mol%) were prepared by melt-quenching technique. It was observed that the density (ρ) decreases, while OPD, molar volume (V_m), and oxygen molar volume (V_o) are nonlinearly varying with the addition of ZnO content from 0 to 30 mol% at the expense of CdO content. From FTIR studies, it is found that the glasses are composed of [BO_4] and [BO_3] units in various borate groups. FTIR and Raman studies revealed that more numbers of BO_4 units are present up to 15 mol% of ZnO, and then with further addition of ZnO in place of CdO up to 30 mol%, most of BO_4 units are converted to BO_3 units. The non-linear variation in T_g is due to the dual role of ZnO. From EPR results, it was found that $g_{\parallel} > g_{\perp}$ and the changes in spin-Hamiltonian parameters are primarily due to the ligand field variations around Cu^{2+} ions. It is found that $g_{\parallel} > g_{\perp} >$ for the present glass system. This suggests that the Cu^{2+} ions in the present glasses are coordinated by six ligands (CuO_6 chromophore) which form an octahedron elongated along the z-axis and also suggests that the ground state of Cu^{2+} ions is the d_{x2-y2} orbital ($^2B_{1g}$ state). From the optical absorption studies, it was found that broad absorption maximum is due to $^2B_{1g} \rightarrow {}^2B_{2g}$ transition of Cu^{2+} ion. The change in polarizability of oxygen ions surrounding the Cu^{2+} could be the reason for the variation of the peak position. The optical absorption results also suggested that there is covalency for the in-plane σ-bonding and that the in-plane π-bonding is significantly ionic in nature in Cu^{2+}–O bonds.

Author details

L.S. Ravangave* and G. N. Devde

*Address all correspondence to: lsravangave@gmail.com

Department of Physics, Shri Sant Gadge Maharaj College, Nanded, Maharashtra, India

References

[1] Cormier L, Majerus O, Neuville DR, Calas G. Temperature-induced structural modification between alkali borate glasses and melts. Journal of the American Ceramic Society. 2006;**89**:13

[2] Yue YL, Yu XJ, Wu HT, Chen XJ. Dielectric properties of quaternary calcium aluminoborosilicate system glasses. Materials Research Innovations. 2009;**13**:129

[3] Shelby JE. Introduction to Glass Science and Technology. Cambridge: The Royal Society of Chemistry; 2005

[4] Abdel-Baki M, El-Diasty F. Role of oxygen on the optical properties of borate glass doped with ZnO. Journal of Solid State Chemistry. 2011;**184**:2762

[5] Hecht HG, Johnston TS. Study of the structure of nickel in soda-boric oxide glasses. The Journal of Chemical Physics. 1967;**46**:23

[6] Devde GN, Upender G, Chandra Mauli V, Ravangave LS. Structure,thermal and spectroscopic properties of Cu^{2+} ions doped $59B_2O_3$-$10K_2O$-(30-x)ZnO-xBaO-1CuO ($0 \leq x \leq 30$ mol%) glass system. Journal of Non-Crystalline Solids. 2016;**432**:319-324

[7] Saddeek, Latif LAE. Effect of TeO_2 on the elastic moduli of sodium borate glasses. Physica B. 2004;**348**:475

[8] Naresh V, Buddhudu S. Structural, thermal, dielectric and ac conductivity properties of lithium fluo-borate optical glasses. Ceramics International. 2012;**38**:2325

[9] Bale S, Rahmana S, Awasthi AM, Sathe V. Role of Bi_2O_3 content on physical, optical and vibrational studies in Bi_2O_3-ZnO-B_2O_3 glasses. Journal of Alloys and Compounds. 2008;**460**:699

[10] Siegel I, Lorence JA. Paramagnetic Resonance of copper in Amorphous and polycrystalline GeO_2. The Journal of Chemical Physics. 1966;**45**:2315

[11] Upender G, Vardhani CP, Suresh S, Awasthi AM, Chandra Mouli V. Structure, physical and thermal properties of WO_3-GeO_2-TeO_2 glasses. Materials Chemistry and Physics. 2010;**121**(1-2):335-341

[12] Upender J, Babu C, Chandra Mouli V. Chandra Mouli,Structure,glass transition temperature and spectroscopic properties of $10LiO_2$-xP_2O_5-(89-x)TeO_2-CuO ($5 \leq x \leq 25$ mol%) glass system. Spectrochimica Acta Part A. 2012;**89**:39

[13] Kamitsos EI, Karakassides MA, Chryssikos GD. Vibrational spectra of magnesium-borate glasses. 2 Raman and mid-infrared investigation of the network structure. Journal of Physical Chemistry. 1987;**91**:1073-1079

[14] Tarte P. In: Prins IA, editor. The determination of cation co-ordination in glasses by infrared spectroscopy. Physics of Non Crystalline Solids. Amsterdam: Elsevier; 1964. p. 549

[15] Condrate RA. The fractography of Glass. In: Pye LD, Stevens HI, Lacourse WC, editors. Introduction to Glass Science. New York: Plenum Press; 1972

[16] Condrate RA. Vibrational spectra of structural units in glass. Journal of Non-Crystalline Solids. 1986;**84**:26

[17] Nelson BN, Exarhos GJ. Vibrational spectroscopy of cation-site interactions in phosphate glasses. Chemical Physics. 1979;**71**:2739

[18] Fayon F, Bessada C, Coutures JP, Massiot D. High Resolution, Double-Quantum 31P MAS NMR Study of the Intermediate-Range order in crystalline and Glass lead phosphate. Inorganic Chemistry. 1999;**38**:5212

[19] El-Damrawi G, El-Egili K. Characterization of novel CeO_2-B_2O_3 glasses. Structure and Properties Physics B. 2001;**299**:180

[20] Abo-Naf M, Azooz MA. Charecterization of some glasses in the system SiO_2-Na_2ORO by infrared spectroscopy. Materials Chemistry and Physics. 2002;**77**:846

[21] Ardelean I, Cora S, Lucacel RC, Hulpus O. EPR,FT-IR, Spectroscopic studies of B_2O_3-Bi_2O_3-MnO glasses. Solid State Sciences. 2005;**7**:1438

[22] Gaafar MS, Saddeek YB, Abd El-Latif L. Ultrosonic studies on alkali borate tungstate glasses. Journal of Physics and Chemistry of Solids. 2009;**70**:173

[23] El-Egili K. Infrared studies of Na_2O-B_2O_3-SiO_2 and Al_2O_3-B_2O_3-SiO_2 glasses. Physica B. 2003;**325**:340

[24] Yiannopoulos YD, Chryssikos GD, Kamitsos EI. Structure and properties of alkaline earth borate glasses. Physics and Chemistry of Glasses. 2001;**42**:164

[25] Dwivedi BP, Rahman MH, Kumar Y, Khanna BN. Raman scattering study of lithium borate glasses. Journal of Physics and Chemistry of Solids. 1993;**54**:621

[26] Furukawa T, White WB. Structure and crystallization of glasses in Li_2O-Si_2O_5-TiO_2 system determined by Raman spectroscopy. Physics and Chemistry of Glasses. 1982;**21**:85

[27] Meera BN, Ramakrishnan J. Raman spectral studies of borate glasses. Journal of Non-Crystalline Solids. 1993;**159**:1

[28] Devde GN, Ravangave LS. Raman, FTIR, DSC, EPR and optical properties of $59B_2O_3$-$10K_2O$-(30-x)ZnO-xLi_2O-1CuO glass system doped with Cu^{2+} ions. IJEST. 2015;**7**(12):407-417

[29] Rejisha SR, Anjana PS, Gopakumar N, Santha N. Synthesis and characterization of strontium and barium bismuth borate glass-ceramics. Journal of Non-Crystalline Solids. 2014;**388**:68

[30] Subhadra M, Kistaiah P. Effect of Bi2O3 content on physical and optical properties of $15Li_2O$-$15K_2O$-xBi_2O_3-(65-x)B_2O_3-$5V_2O_5$ glass system. Vibrational Spectroscopy. 2012;**62**:23

[31] Sekiya T, Mochida N, Ohtsuka A, Soejima A. Raman spectra of BO3/2-TeO2 glasses. Journal of Non-Crystalline Solids. 1992;**151**:222

[32] Ciceo-Lucacel R, Ardelean I. FT-IR and Raman study of silver lead borate-based glasses. Journal of Non-Crystalline Solids. 2007;**353**:2020

[33] Upendre G, Chandramouli VC, Prasad M. Vibrational, EPR and Optical Spectroscopy of Cu^{2+} doped glasses with$(90\text{-}x)TeO_2\text{-}10GeO_2\text{-}xWO_3(7.5 \leq x \leq 30$ mol%) composition. Journal of Non-Crystalline Solids. 2011;**357**(3):903-909

[34] Dimitrov V, Komatsu T. An interpretation of optical properties of oxides and oxide glasses interms of electronic ion polarizability and average single bond length. Journal of Chemical Technology and Metallurgy. 2010;**45**:219

[35] Volf B. Chemical Approach to Glass. New York: Elsevier; 1984

[36] Ramesh Kumar V, Rao JL, Gopal NO. EPR and optical absorption studies of Cu^{2+} ions in alkaline earth alumino borate glasses. Material Research Bulletin; 2005;**40**:1256-1269

[37] Srinivasulu K, Omkaram I, Obeid H, Suresh Kumar A, Rao JL. Spectral studies of Cu^{2+} ions in sodium-lead borophosphate glasses. Physica B. 2012;**407**:4741

[38] Kivelson D, Neiman R. ESR Line shapes in glasses of copper complexes. The Journal of Chemical Physics. 1961;**35**:145

[39] Abdel-Baki M, Abdel-Wahab FA, El-Diasty F. One-Photon band gap engineering of borate glass doped with ZnO for photonic application. Journal of Applied Physics. 2012;**111**. DOI: 073506